J Fluoresc (2007) 17:377–382
DOI 10.1007/s10895-007-0204-2

ORIGINAL PAPER

Fluorescence Modulation of Acridine and Coumarin Dyes by Silver Nanoparticles

Carolina A. Sabatini · Robson V. Pereira · Marcelo H. Gehlen

Received: 26 January 2007 / Accepted: 4 May 2007 / Published online: 5 June 2007

Abstract Silver nanoparticles were synthesized by chemical reduction of silver ions by sodium borohydride in the presence of poly-(*N*)-vinyl-2-pyrrolidone in solution of short chain alcohols. The nanoparticles are stable in 2-propanol, and the average diameter of the Ag colloid obtained in this solvent is about 6 nm. The photophysical properties of acridinium and coumarin dyes in 2-propanol are affected by the presence of silver nanoparticles. The interaction of silver nanoparticles with acridinium derivative leads to a spectral change of its intramolecular charge transfer (ICT) absorption band. The dye emission increases suddenly with the initial addition of the Ag metal nanoparticles, but at a high concentration of the colloid, static fluorescence quenching occurs with a progressive decrease of the fluorescence efficiency. Amino coumarin fluorescence is only quenched by the silver nanoparticles in solution.

Keywords Silver nanoparticles · Dyes · Fluorescence · Plasmon resonance · ICT

Introduction

Metal nanoparticles have attracted significant attention due to their interesting optical and electronics properties, which have resulted in the exploitation of a number of applications in chemistry and in biochemistry [1–6]. Particularly, the resonance plasmon effect in photophysical properties of organic chromophores like dyes is still an intricate phenomenon [7]. The type, size and shape of the nanoparticles can modulate the fluorescence of a target dye close to the metal surface. The enhancement of the fluorescence efficiency due to the electronic coupling of the electronic transition dipole moment with surface plasmons is a desired effect owing the use of medium to low-quantum yield fluorophores in molecular probing devices [8–11].

The synthesis of silver nanoparticles can be performed by chemical reduction of silver ions by sodium borohydride in aqueous phase [12]. Advanced preparation methods have been carried out in organic solvents to increase stability of formed particles, because in aqueous phase silver particles tend to aggregate. Within that scope, ingenious ways have been developed where nanoparticles are transferred from aqueous to organic phase. Generally, phase transfer of metal nanoparticles between aqueous phase and organic phase needs two additives: one is the stabilizer of nanoparticles, and the other is the phase transfer agent [13, 14].

In many cases, nanoparticles are surface modified by adsorption of alkanethiol or fatty acid molecules, but only in a few reports the phase transfer of nanoparticles is obtained by complexation with long chain amines. For instance, colloidal silver nanoparticles synthesized in water can be quantitatively transferred to hexane by direct coordination with octadecylamine molecules present in the organic phase [14].

However, these methods of transferring nanoparticles from aqueous to organic phase have disadvantages for requiring elaborate procedures, and some of the additives like amines and thiols are fluorescence quenchers of many dyes. Considering this, silver nanoparticles are prepared in alcohols, eliminating the transfer step. They are synthesized by chemical reduction of silver nitrate by sodium borohydride, in the presence of stabilizing poly-(*N*)-vinyl-2-pyrrolidone (PVP) in solution of short chain alcohols. The fluorescence behavior of two classes of dye, coumarin

C. A. Sabatini · R. V. Pereira · M. H. Gehlen (✉)
Instituto de Química de São Carlos, Universidade de São Paulo, 13566-590 São Carlos, SP, Brazil
e-mail: marcelog@iqsc.usp.br

and acridine, both with intramolecular charge transfer (ICT) character, are then studied in the presence of silver colloids in solution.

Materials and methods

Silver nanoparticles were prepared in a series of alcohols (methanol, ethanol, *n*-propanol, 2-propanol, butanol, *t*-butanol) by chemical reduction of silver ions ($AgNO_3$; from J. T. Baker) by sodium borohydride ($NaBH_4$; from Vetec) in the presence poly-(*N*-vinyl-2-pyrrolidone) (PVP; Mw=1,300 kg mol^{-1} from Aldrich). In the preparation, 10 ml 1.0 mM of $AgNO_3$ in alcoholic solution was added to 10 ml 5.0 mM of $NaBH_4$, under stirring in the presence of PVP used as stabilizing agent. The preparation was made in ice bath and with protection from light. The formation of silver nanoparticles was confirmed by absorption spectroscopy of the yellow solution obtained.

The acridinium derivatives I, II and III (see the molecular structure of the dyes used in Fig. 1) were synthesized in our group as given elsewhere [15, 16]. The amino coumarin (C1, C151, C500) were purchased from Acros Organics, and the C120 from Sigma. The alcohols were dried in molecular sieves before their use.

The absorption measurements were carried out on a Cary 5G Varian spectrophotometer, and the steady-state fluorescence spectra were obtained using a Hitachi F-4500 spectrofluorometer. Fluorescence decays were measured in solution by time correlate single photon counting technique using a CD-900 Edinburgh spectrometer. The light pulse was provided by frequency doubling the laser pulse of Mira 900 Ti/sapphire pumped by Verdi 5W from Coherent. The fluorescence decays were analyzed by a reconvolution procedure using exponential decays models. All fluorescence measurements were performed using front-face irradiation and detection. The transmission electron microscopy images were obtained on a Philips CM200 microscope operated at acceleration tension of 200 kV and line resolution of 0.144 nm, and the silver nanoparticles were impregnated in copper grid for analysis.

Results and discussion

The preparation of silver nanoparticles in a series of alcohols was promptly achieved by the chemical reduction step. The tested alcohols were methanol, ethanol, *n*-propanol, 2-propanol, butanol and *t*-butanol. The solution of formed silver nanoparticles in these alcohols was monitored by electronic absorption to control the size of silver nanoparticles and the colloid stability. The results showed that the more stable Ag colloids were obtained in 2-propanol, where the Ag colloid absorption spectrum remained constant over days.

In alcoholic solution, the absorption maximum of the Ag nanoparticles is red shifted in about 10 to 12 nm compared to the colloid prepared in water. This difference is illustrated with the absorption profiles given in Fig. 2. The reason of the red shift as well as of the broadening of the absorption band could be the presence of asymmetrical particles with long and short axis like prolate spheroids and nanorods [17]. Nevertheless, the average radius of Ag nanoparticles may be estimated from the electronic spectrum using an approximation within the scope of the Mie-Drude theory as given by the following equation:

$$R = \frac{v_F}{\Delta\omega_{1/2}} \tag{1}$$

where $\Delta\omega_{1/2}$ is the width of half height of the absorption maximum, and v_F the Fermi velocity (1.39×10^8 cm s^{-1}) [18]. The average radius of silver nanoparticles in 2-propanol

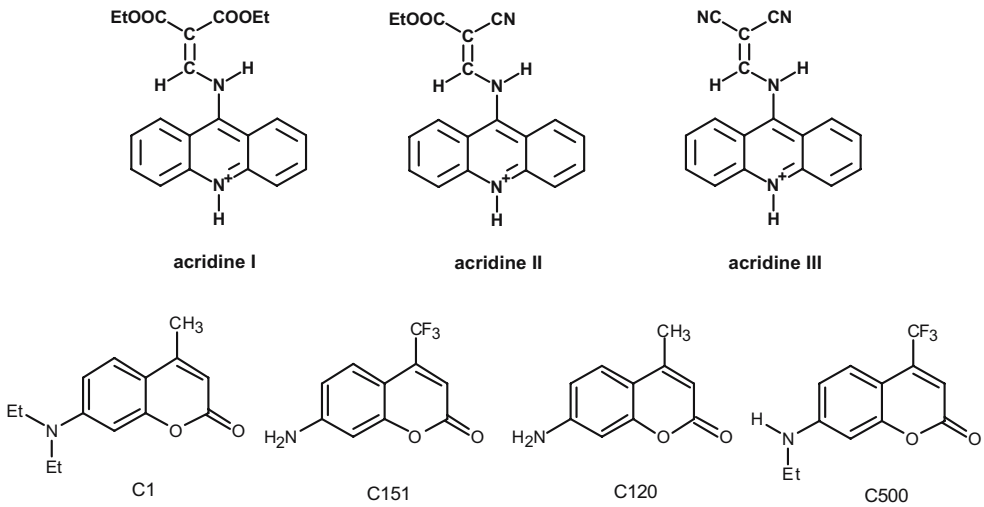

Fig. 1 Chemical structures of the acridinium (I, II, and III) and amino coumarin (C1, C151, C120, and C500)

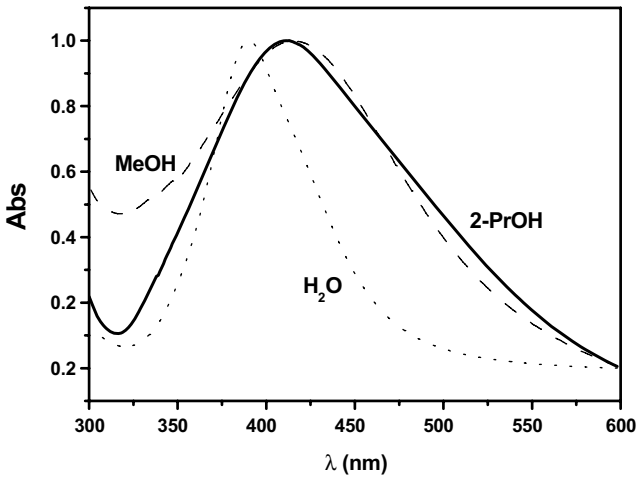

Fig. 2 Comparison between normalize absorption spectra of silver nanoparticles prepared in water, in 2-propanol, and in methanol

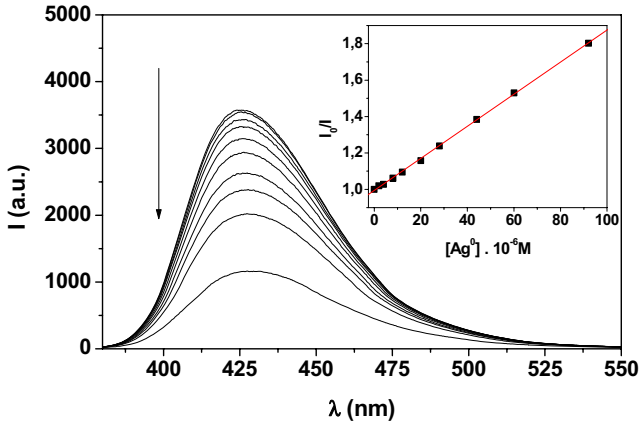

Fig. 4 Fluorescence spectra of C120 in 2-propanol (λ_{ex}=350 nm) upon addition of Ag nanoparticles. [Ag^0] from 0–9.2×10^{-5} M. Stern–Volmer analysis (*inset*) gives a linear parameter 0.994±0.003 and correlation coefficient of 0.99

is estimated in 6 nm while the nanoparticles prepared in water have a radius of about 11 nm, from Mie–Drude theory.

The transmission electron microscopy image revealed that average radius of silver nanoparticles obtained in 2-propanol is approximately 5–6 nm, in agreement with result obtained by absorption spectroscopy. A typical image is represented in the Fig. 3.

The photophysics properties of the amino coumarin and of the acridinium derivatives are modulated by the presence of silver nanoparticles in 2-propanol. These systems were studied by stationary and time resolved fluorescence measurements. The concentration of silver nanoparticles was varied from 0 up to about 200 μM, with regard to analytical concentration of Ag^0.

The fluorescence of the amino coumarin dyes is only quenched by the Ag nanoparticles. A typical spectral quenching data is given in Fig. 4 for the case of C120.

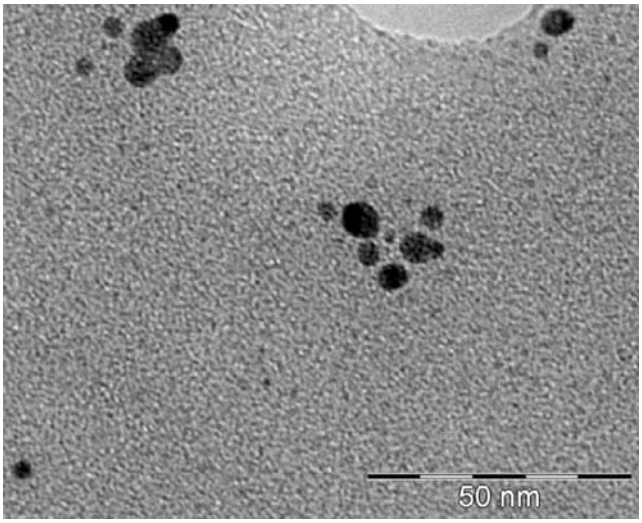

Fig. 3 TEM image of silver nanoparticles obtained in 2-propanol

For this dye, the Stern–Volmer analysis provides a K_{SV} of 8,810 M^{-1}.

For the other coumarins C1, C151 and C500, fluorescence quenching is also observed, but their Stern–Volmer plots were no longer linear (see Fig. 5).

The linear term at low [Ag^0] may be ascribed to the Stern–Volmer constant (K_{SV}), and the calculated results are reported in Table 1. The decays of the amino coumarins in 2-propanol were monoexponential (lifetimes are listed in Table 1). However, these lifetimes of the dyes did not change upon addition of the Ag colloid. This indicates that the quenching observed in steady state measurements is considered static [19]. In fact, using the K_{SV} constants and lifetimes, the required bimolecular quenching rate constant will be larger than 10^{12} M^{-1} s^{-1} overcoming the diffusion

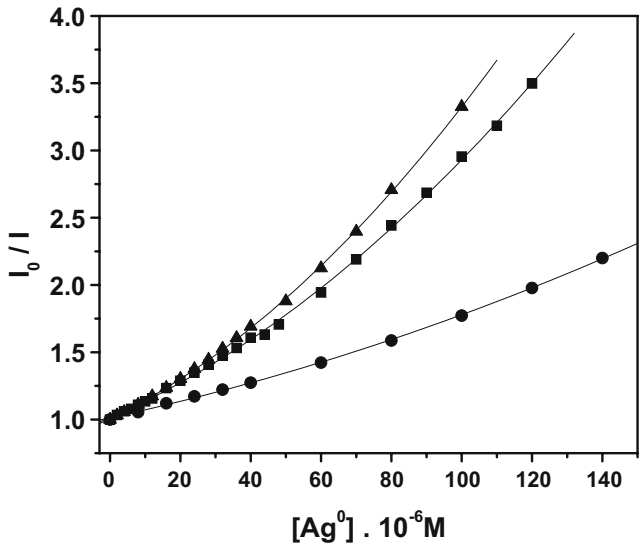

Fig. 5 Stern–Volmer plot of coumarin in 2-propanol, (*triangle* C1), (*square* C151), (*circle* C500). Correlation coefficient of the polynomial fit is 0.99 in the three cases and linear parameter is near one

controlled rate limit in this solvent. This static quenching could be ascribed to an association of the coumarin with the Ag nanoparticle through complexation of the metal with its amino group. In this case, a single Ag nanoparticle would be able to complex more than a single dye, and thus the remaining fraction of free dyes in solution will decreases as the concentration of Ag colloid is increased. However, if the occupancy of the dye among the nanoparticles follows an ideal Poisson statistics like that in classical solute partitioning and fluorescence quenching in micelles [20], the relative intensity I_0/I will scale linearly with concentration of Ag colloid, and the K_{SV} constant will correspond to the association constant. Bound to the metal surface, the dye has a complete quenching by very fast energy transfer given then the static behavior found. This model still does not explain the upward curvature observed, and such effect could be related to a larger quenching sphere of action [19] due to the long range dipole–dipole interaction of the metal nanoparticle with any dye molecule close to the surface, but not fully associated. Also, amino coumarin may form an intramolecular charge transfer state upon light excitation (TICT molecule) [21]. Its hydrogen bonding capacity [22] allied to efficiently and fast nonradiative deactivation of its ICT state in polar protic environments, would also contribute to the static quenching in PVP covered Ag nanoparticles.

The value of lifetime τ_1 found for C1 in 2-propanol (3.5 ns listed in Table 1) corresponds very well with the reported values in alcohols [21], but for C151 and C500 the respective lifetimes of 5.3 and 5.7 ns are slightly higher than reported values of 4.5 and 4.6 ns found in $CHCl_3$ solution [22].

With regard to the acridine derivatives (acridine I, II, III), it was also observed the modulation in their photophysics properties by silver nanoparticles in 2-propanol solution. For compound I, only fluorescence quenching upon addition of silver nanoparticles is observed. The Stern–Volmer plot was linear, and from it, the K_{SV}=6,690 M^{-1} is obtained, a value within the range of those previously calculated for coumarins. Again, the fluorescence quenching of acridine I is a static quenching process, considering that lifetimes of the dye remained constant with concentration of added Ag colloid. The three acridine derivatives, however, are dyes with biexponential decay behavior even in pure solvent, a behavior ascribed to an interconversion between locally excited single (LE) state and intramolecular charge transfer (ICT) state [15, 16]. The formation of ICT state is related to the presence of the electron withdrawing group like CN and *C=O* in the aminovinyl substituent of the acridine fluorophore. The decay time τ_1 is related to the ICT emission with the larger contribution % while the decay τ_2 is ascribed mainly to the fraction of dye emitting from LE state.

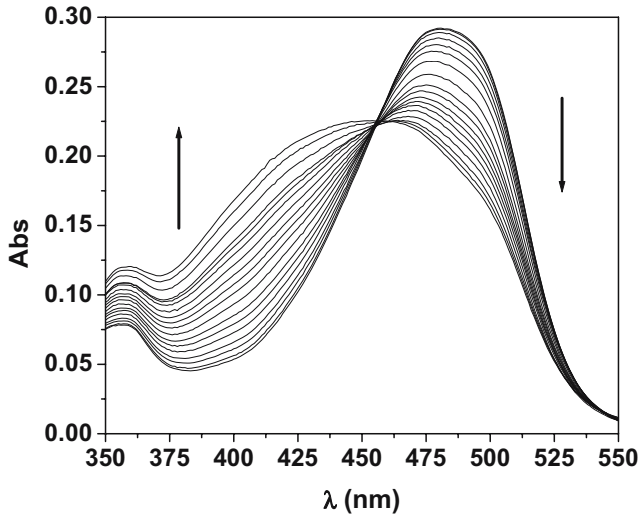

Fig. 6 Absorption spectra of acridine II in 2-propanol with addition of silver nanoparticles. [Ag^0] from 0–1.4×10^{-4} M

Contrasting with the behavior of acridine I, compounds II and III have their absorption spectra changed by addition of Ag colloid. For instance, the absorption spectra of acridine II upon addition of Ag colloid are given in Fig. 6. The presence of an isosbestic point at 458 nm may indicate of the presence two species in equilibrium. Considering the already reported association of acridinium with Ag colloid by strong interaction of the endocyclic N of the chromophore with deprotonation of the dye [23], the two species in our case could be the free acridinium derivative in solution (with optical ICT band with maximum at 480 nm) and the deprotonated dye adsorbed on the Ag colloid with absorption spectrum more in the blue region.

Table 1 Stern–Volmer constant (K_{SV}), lifetime (τ) and emission maximum of the fluorescence of the dyes in 2-propanol/Ag^0

Concentrations: acridine 2×10^{-5} M, coumarin 3.7×10^{-5} M. Excitation at 401 nm.

Dyes	K_{SV} (M^{-1})	τ_1 (ns)	Rel (%)	τ_2 (ns)	Rel (%)	λ_{em} (nm)
C1	12,600	3.5	100	–	–	445
C120	8,810	4.1	100	–	–	425
C151	11,400	5.3	100	–	–	475
C500	5,800	5.7	100	–	–	490
Acridine I	6,690	2.2	97	6.3	3	470
Acridine II	825	1.4	94	8.0	6	525
Acridine III	660	1.4	91	8.5	9	520

The compounds II and III also showed a different behavior compared to compound I with respect to the fluorescence intensity. The main difference is that compound II and III have a fluorescence intensity enhancement upon addition of a small amount of Ag colloid, and quenching occurs only at a higher concentration of nanoparticles. This dual behavior is well illustrated in the case of compound II with addition of Ag colloid as given in Fig. 7. When the excitation is performed at the isosbestic point, where the optical density remains constant, the dual behavior of the ICT emission still appear.

In order to compare the dual effect for these compounds, the relative integrated intensity as a function of Ag colloid concentration is plotted in Fig. 8. The initial enhancement of relative fluorescence is about a factor 6 and 2.5 for compounds II and III, respectively. As the fluorescence quantum yield of these compounds are lower than 0.1 [15, 16], the fluorescence enhancement could be due to a plasmon resonance effect over the ICT excited state promoting an increase of its radiative rate constant (metal plasmon-coupled emission effect [24]), and therefore, the enhancement of the fluorescence efficiency. However, our time resolved experiments have indicated a practically constant decay time components of these dyes with concentration of Ag colloid, (i.e. the average lifetime was also constant). Thus, if such effect occurs, then it should be minimal in this case.

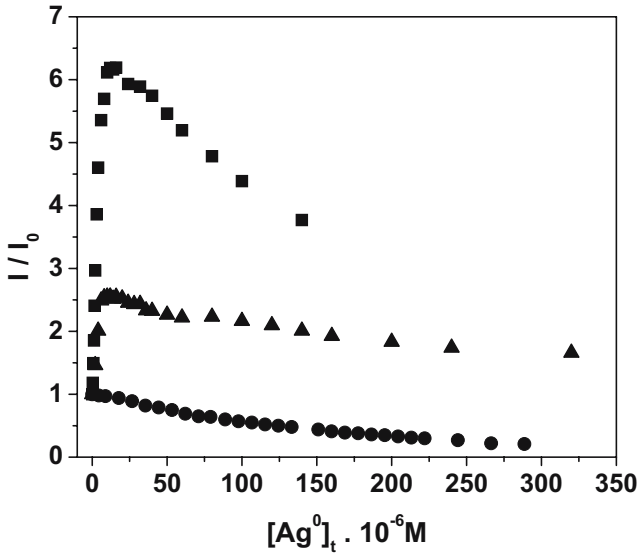

Fig. 8 Comparison of the increase between acridine II (*square*) and acridine III (*triangle*) and decrease of acridine I (*circle*) stationary fluorescence

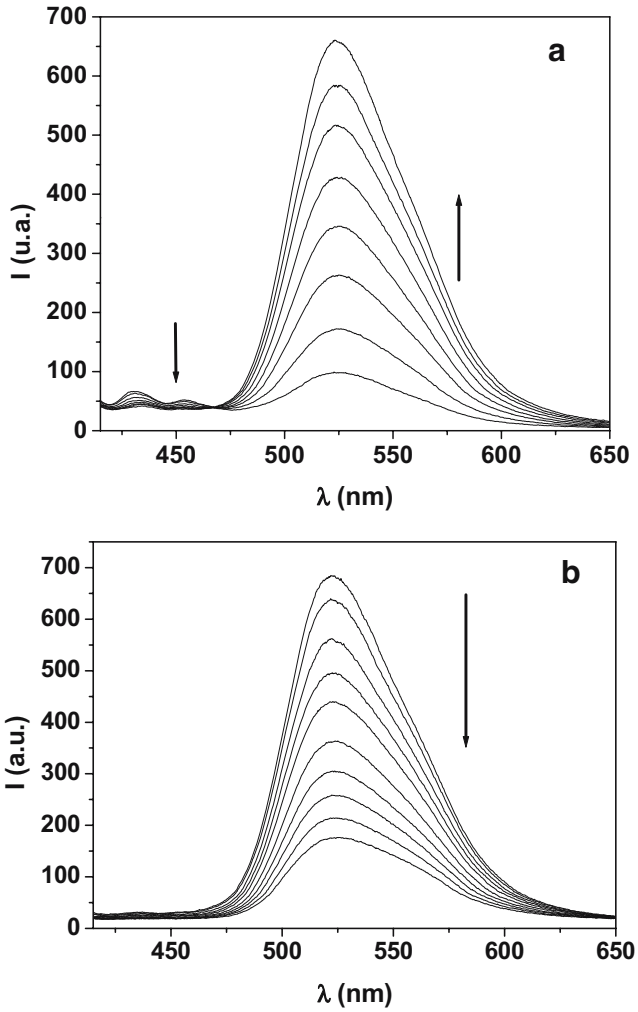

Fig. 7 Fluorescence intensity enhancement (**a**) and quenching (**b**) of acridine II with addition of Ag colloid in 2-propanol. [Ag^0]: **a** 0–1.2×10^{-5} M, and **b** 1.4–14×10^{-5} M

The unexpected effect, however, is the quenching of the LE emission (the weak structured band at about 450 nm) in all concentration range (see Fig. 7a, excitation is at 400 nm). It seems that the enhancement in fluorescence intensity is related to a fast interconversion of S_1 to ICT excited state which will not result in an appreciable change of the ICT lifetime, but it will increase the population of the ICT excited state, and therefore, providing a channel to higher fluorescence efficiency of the red emission band as observed. Another point is that the added Ag colloid solution is a slightly basic solution due to the presence of remained borohydride and borate side product of the preparation. These anions may be partially associated with PVP polymer and thus will assist in the deprotonation of the dye near the colloid Ag as discussed before. Nevertheless, at the higher concentration of Ag colloid, quenching dominates, and from the decrease of the relative fluorescence intensity, an apparent Stern–Volmer constants may be evaluated for acridine II and III as 825 M^{-1} and 660 M^{-1}, respectively. These values are one order of magnitude lower than those values observed for the other dyes as reported in Table 1.

The higher overlap of the absorption spectrum of the Ag nanoparticles with the emission spectra of coumarins (data not shown) predicts a more efficient energy transfer for these dyes. This fact is in accordance with the observed higher fluorescence quenching of coumarins with increase of the concentration of Ag nanoparticle when compared with the quenching of acridines.

Conclusions

The acridine and amino coumarin derivatives have their fluorescence changed by the presence of low concentration of Ag nanoparticles stabilized by PVP in 2-propanol. The fluorescence quenching with a static behavior seems to occur as a result of the binding of the dyes onto the surface of the nanoparticles, providing a fast and efficient path to excited state nonradiative deactivation. The dual behavior found for two of the acridine derivatives, where the initial addition of Ag nanoparticles produces an apparent enhancement of the emission efficiency of the ICT, is ascribed to a larger yield formation of ICT excited state in the Ag colloid solution and not to metal plasmon-coupled emission with the dye excited state.

References

1. Kamat PV (2002) Photophysical, photochemical and photocatalytic aspects of metal nanoparticles. J Phys Chem B 106: 7729–7744
2. Lakowicz JR (2001) Radiative decay engineering. Anal Biochem 298:1–24
3. Lakowicz JR, Shen Y, D'Auria S, Malicka J, Fang J, Gryczynski Z, Gryczynski I (2002) Radiative decay engineering: 2. Effects of silver islands films on fluorescence intensity, lifetimes, and resonance energy transfer. Anal Biochem 301:261–277
4. Lakowicz JR (2004) Radiative decay engineering 3. Surface plasmon-coupled directional emission. Anal Biochem 324: 153–169
5. Aslan K, Cryczynski I, Malicka J, Lakowicz JR, Geddes CD (2005) Metal-enhanced fluorescence: an emerging tool in biotechnology. Curr Opin Biotechnol 16(1):55–62
6. Aslan K, Holley P, Davies L, Lakowicz JR, Geddes CD (2005) Angular-ratiometric plasmon-resonance based light scattering for bioaffinity. J Am Chem Soc 127:12115–12121
7. Aslan K, Malyn SN, Geddes CD (2007) Metal-enhanced fluorescence from gold surfaces: angular dependent emission. J Fluoresc 17:7–13
8. Zhang J, Matveeva E, Gryczynski I, Leonenko Z, Lakowicz JR (2005) Metal-enhanced fluoroimmunoassay on a silver film by vapor deposition. J Phys Chem B 109:7969–7975
9. Zhang J, Malicka J, Gryczynski I, Lakowicz JR (2005) Surface-enhanced fluorescence of fluorescein-labeled oligonucleotides capped on silver nanoparticles. J Phys Chem B 109:7643–7648
10. Corrigan TD, Guo S, Phaneuf RJ, Szmacinski H (2005) Enhanced fluorescence from periodic arrays of silver nanoparticles. J Fluoresc 15:777–784
11. Haes AJ, Stuart DA, Nie S, Van Duyne RP (2004) Using solution-phase nanoparticles, surface-confined nanoparticle arrays and single nanoparticles as biological sensing platforms. J Fluoresc 14:355–367
12. Machulek Junior A, De Oliveira HPM, Gehlen MH (2003) Preparation of silver nanoprisms using poly(*N*-vinyl-2-pyrrolidone) as a colloid stabilizing agent and the effect of silver nanoparticles on the photophysical properties of cationic dyes. Photochem Photobiol Sci 2:921–925
13. Zhao SY, Chen SH, Li DG, Yang XG, Ma HY (2004) A convenient phase transfer route for Ag nanoparticles. Physica E 23:92–96
14. Kumar A, Joshi H, Pasricha R, Mandale AB, Sastry M (2003) Phase transfer of silver nanoparticles from aqueous to organic solutions using fatty amine molecules. J Colloid Interface Sci 264:396–401
15. Pereira RV, Ferreira APG, Gehlen MH (2005) Excited-state intramolecular charge transfer in 9-aminoacridine derivative. J Phys Chem A 109:5978–5983
16. Pereira RV, Gehlen MH (2006) Photoinduced intramolecular charge transfer in 9-aminoacridinium derivatives assisted by intramolecular H-bond. J Phys Chem A 110:7539–7546
17. Hao E, Schatz GC, Hupp JT (2004) Synthesis and optical properties of anisotropic metal nanoparticles. J Fluoresc 14: 331–341
18. Haykawa T, Selvan ST, Nogami M (1999) Enhanced fluorescence from Eu^{+3} owing to surface plasma oscillation of silver particles in glass. J Non-Cryst Solids 259:16–22
19. Lakowicz JR (1999) Principles of fluorescence spectroscopy, 2nd edn. Kluwer, New York, chapter 8
20. Gehlen MH, De Schryver FC (1993) Time resolved fluorescence quenching in micellar assemblies. Chem Rev 93:199–221
21. Barik A, Kumbhakar M, Nath S, Pal H (2005) Evidence for the TICT mediated nonradiative deexcitation process for the excited coumarin-1 dye in high polarity protic solvents. Chem Phys 315:277–285
22. Das H, Jain B, Patel HS (2006) Hydrogen bonding properties of coumarin 151, 500 and 35: the effect of substitution at 7-amino position. J Phys Chem A 110:1698–1704
23. Rivas L, Murza A, Sánchez-Cortés S, García-Ramos JV (2001) Adsorption of acridine drugs on silver surface-enhanced resonance Raman evidence of the existence of different adsorption sites. Vibr Spectrosc 25:19–28
24. Aslan K, Leonenko Z, Lakowicz JR, Geddes CD (2005) Annealed silver-island films for applications in metal-enhanced fluorescence: interpretation in terms of radiating plasmons. J Fluoresc 15:643–654